Tunable THz Leaky-Wave Radiation from Periodic Chains of Graphene-Coated Circular Rods

Lorenzo Cioci, Vakhtang Jandieri, *Senior Member, IEEE*, Walter Fuscaldo, *Senior Member, IEEE*, Paolo Burghignoli, *Senior Member, IEEE*, and Paolo Baccarelli, *Member IEEE*

***Abstract*—The beam-scanning properties at a fixed frequency in the low terahertz range of one-dimensional periodic leaky-wave antennas composed by a periodic chain of circular dielectric cylinders coated with graphene are studied. A rigorous full-wave modal solver, based on the lattice-sums technique combined with the transition-matrix approach, is applied to the analysis of transverse electric (TE) and magnetic (TM) leaky modes, where the transition matrix suitably takes into account the conductivity of the external graphene sheet. The reconfigurable features of the leaky-wave structure have been investigated in terms of the dispersion behaviors of the phase and attenuation constants of the radiating proper $n = -1$ space harmonic of the Bloch leaky modes. The beam-scanning performance, variation of the beamwidth, and the appearance of grating lobes as functions of the graphene chemical potential are investigated. Three-dimensional structures composed by a finite number of graphene-coated dielectric rods sandwiched by metal or perfect magnetic conductor plates are finally validated through full-wave simulations, showing a good beam-scanning capability for both TE and TM polarizations, respectively, and a remarkable agreement with the theoretical leaky-wave model.**

***Index Terms*—Leaky-wave antenna, periodic structure, beam scanning, graphene, tunable antenna.**

I. INTRODUCTION

TUNABLE leaky-wave antennas (LWAs) using graphene to dynamically steer the beam at a fixed terahertz (THz) frequency, have attracted specific attention in the last decade for applications in diverse scenarios, from sensing and quality control to imaging and wireless communications [1]–[5]. Both plasmonic and nonplasmonic configurations have been investigated, where the former have shown excellent performance in terms of tunable beamscanning features [1], [6], and the latter have been found particularly efficient in reducing the undesired effects of the intrinsic ohmic losses of graphene [3], [7], [8]. Different graphene open waveguides based on printed or dielectric structures have been recently investigated in terms of plasmonic or other *exotic* guiding properties [9]. A particular interest has been devoted to graphene-coated dielectric-rod (GCDR) waveguides and various promising devices have been proposed and in a few cases experimentally demonstrated [10]–[14]. Dispersion features of complex waves propagating along GCDRs [15] and plasmonic LWAs based on GCDR with sinusoidally modulated radius or reactance surface [16], [17] have been studied.

L. Cioci and P. Baccarelli are with the Department of Industrial, Electronic, and Mechanical Engineering, Roma Tre University, 00146 Rome, Italy. (e-mail: lor.cioci@gmail.com; paolo.baccarelli@uniroma3.it).

V. Jandieri is with the Department of General and Theoretical Electrical Engineering (ATE), Faculty of Engineering, University of Duisburg–Essen, 47048 Duisburg, Germany, and also with the Center for Nanointegration Duisburg–Essen (CENIDE), 47048 Duisburg, Germany.(e-mail: vakhtang.jandieri@uni-due.de).

W. Fuscaldo is with the “Istituto per la Microelettronica e Microsistemi”, Consiglio Nazionale delle Ricerche, 00133 Rome, Italy.(e-mail: walter.fuscaldo@artov.imm.cnr.it).

P. Burghignoli is with the Department of Information Engineering, Electronics and Telecommunications, “Sapienza” University of Rome, 00184 Rome, Italy. (e-mail: paolo.burghignoli@uniroma1.it).

This work was supported by Shota Rustaveli National Science Foundation of Georgia (SRNSFG) [FR-23-249].

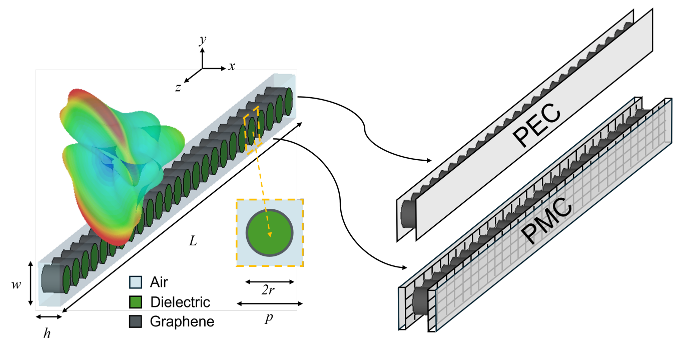

Fig. 1. Periodic chain of 2-D graphene coated dielectric circular rods in free space. The period of the structure is p, the relative dielectric permittivity and the radius of the dielectric rods are ϵ_r and r, respectively. Graphene is characterized by a complex conductivity σ defined by (4).

The possibility of exploiting periodicity in conjunction with the use of graphene is of great interest in LWA design [1], [6], [18]. In fact, periodic open waveguides allow for obtaining beams that can point in the backward as well as in the forward quadrants of the LWA, by varying frequency or the physical parameters of the material [19], [20]. The use of graphene as a periodic perturbation of an open waveguide allows for varying the periodic load either uniformly on the entire structure, or selectively by acting independently on each cell of the linear array. This provides in principle not only for scanning the directive beam at a fixed frequency, but also for tapering the LWA for beam shaping. These performance are needed in dynamic contexts, as those of mobile communications at THz, that require antenna technologies offering high directivity and a reconfigurable feature. LWAs could provide a solution to these issues, also considering that phased arrays at THz do not represent a viable technology.

In this Letter, a self-contained full-wave modal formulation based on the Lattice-Sums (LSs) technique combined with the T-matrix approach [21], [22] has been adapted to study for the first time the propagation of leaky modes in periodic chains of two-dimensional (2-D) GCDRs, whose geometrical configuration is completely different from the leaky cylindrical waveguides studied in [16], [17]. The T-matrix, which is available in a closed form for the circular dielectric rod [23], has been suitably modified for considering an external graphene coating layer, whose conductivity is modeled with the Kubo formula (neglecting nonlocal effects) [24]. The dispersion behavior of the normalized phase and attenuation constants of the $n = -1$ space harmonic of the fundamental transverse electric (TE) and magnetic (TM) leaky modes of the considered periodic chain are studied by varying the chemical potential of graphene. Limits and potentialities of this tunable leaky-wave configuration are investigated in terms of scanning angle ranges, beamwidth deformation, and grating-lobe occurrence by varying the physical parameters of graphene. The simulation of three-dimensional (3-D) LWAs realized by a finite number of GCDRs sandwiched between perfect electric or magnetic conductor plates (PEC or PMC, respectively) fully validates the theoretical predictions based on the 2-D full-wave leaky modal approach. The capability to scan the beam of about 10° while maintaining directivities higher than 10 dB with a change of only a few tenths of electronvolts confirms the great sensitivity of this structure. This is a remarkable property in the context of graphene-based LWAs, which may open interesting perspectives for emerging THz applications.

II. Periodic Chain of GCDRs

The structure composed of periodically distributed GCDRs with circular section having a radius r and a relative dielectric permittivity ϵ_r is demonstrated in Fig. 1. It is geometrically invariant along the x-axis and infinite and periodic with a period p along the z-axis. The surrounding medium is free space with permittivity ϵ_0 and permeability μ_0. Applying addition theorem for the cylindrical functions, a simple dispersion equation for the eigenmodes is obtained in the following form:

$$\det[\mathbf{I} - \mathbf{T}(k_0 r)\mathbf{L}(k_0 p, k_{x0} p)] = 0 \quad (1)$$

where $\mathbf{I}$ is the unit matrix. The T-matrix of a GCDR, which describes the nature of the scatterer per unit cell, can easily be written in terms of a diagonal matrix and it is given for the TM wave (H_x, E_z, E_y) and the TE wave (E_x, H_z, H_y) as:

$$T_m^{\mathrm{TM}} = \frac{-J_m \tilde{J}_m' + \sqrt{\epsilon_r} J_m' \tilde{J}_m - j\sigma\sqrt{(\mu_0/\epsilon_0)} J_m' \tilde{J}_m'}{H_m^{(2)} \tilde{J}_m' - \sqrt{\epsilon_r} H_m^{(2)'} \tilde{J}_m + j\sigma\sqrt{(\mu_0/\epsilon_0)} H_m^{(2)'} \tilde{J}_m'} \quad (2)$$

$$T_m^{\mathrm{TE}} = \frac{-\tilde{J}_m J_m' + \sqrt{\epsilon_r} J_m \tilde{J}_m' + j\sigma\sqrt{(\mu_0/\epsilon_0)} J_m \tilde{J}_m}{H_m^{(2)'} \tilde{J}_m - \sqrt{\epsilon_r} H_m^{(2)} \tilde{J}_m' - j\sigma\sqrt{(\mu_0/\epsilon_0)} H_m^{(2)} \tilde{J}_m}. \quad (3)$$

Here $J_m := J_m(k_0 r)$, $\tilde{J}_m := J_m(k_1 r)$, and $H_m^{(2)} := H_m^{(2)}(k_0 r)$ are Bessel and Hankel functions of the m-th order, respectively, the prime notation denotes their derivatives with respect to the arguments, $k_0 = \omega\sqrt{\mu_0\epsilon_0}$ and $k_1 = \omega\sqrt{\mu_0\epsilon_0\epsilon_r}$, ω is the angular frequency, and σ is the graphene complex conductivity. When $\sigma \to 0$, (2) and (3) reduce to the T-matrix expression for a dielectric rod per unit cell [23]. The graphene complex conductivity σ that appears in (2) and (3) is well approximated by the intraband contributions of Kubo formula in the low THz regime [8], [24]:

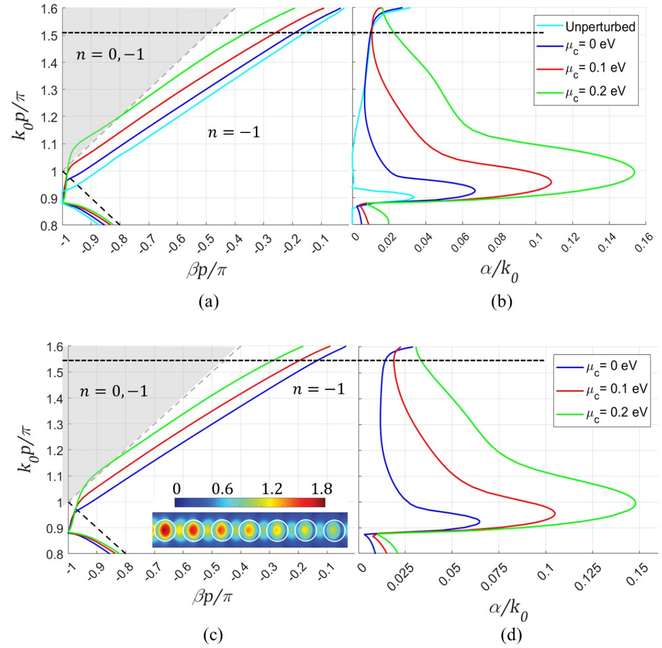

Fig. 2. Brillouin diagram for the fundamental TM leaky mode of the periodic chain of GCDRs (Fig. 1) with $\epsilon_r = 2.25$ and $r = 0.4167p$. (a) and (c) normalized phase constant $\beta p/\pi$ of the $n = -1$ space-harmonic vs. normalized frequency $k_0 p/\pi$ for $\tau = 1$ ps and $\tau = 0.5$ ps, respectively; (b) and (d) the relevant normalized attenuation constant α/k_0. Three different values of the chemical potential $\mu_c = 0, 0.1, 0.2$ eV are plotted by the blue, red, and green lines, respectively. The result for pure dielectric rods (unperturbed rods, without graphene coating) is also shown with a cyan line. The light line and their replicas are shown by the black and gray dashed oblique lines, respectively. The shadowed areas show the region where the $n = 0$ and $n = -1$ harmonics are simultaneously radiating. The horizontal black dashed lines indicate operating frequencies. In (c) the amplitude of the H_x leaky modal field is reported for $\mu_c = 0.1$ eV at the operating frequency; white circles represent the boundaries of the first seven circular rods.

$$\sigma = \frac{2\tau}{1 + j\omega\tau} \frac{e^2 k_B T}{\pi\hbar^2} \ln\left[2\cosh\left(\frac{\mu_c}{2k_B T}\right)\right] \quad (4)$$

where e is the electron charge, $\hbar$ is the reduced Plank constant, k_B is the Boltzmann constant, T is the temperature, μ_c is the chemical potential, τ is the relaxation time of graphene. Here, ideal relaxation time of 1 ps, as also adopted in [16], [17], and a more realistic value of 0.5 ps are used to model the graphene layer [25].

The LSs ($\mathbf{L}$-matrix) in (1) play a key role in our formalism and an accelerated and effective numerical evaluation has been proposed in [21], [22]. The modal field in a periodic chain of GCDRs can be expressed in terms of an infinite series of space harmonics, each having a complex propagation wavenumber $k_{zn} = \beta_n - j\alpha$, with $\beta_n = \beta_0 + 2\pi n/p$ and $n = 0, \pm 1, \pm 2, \cdots$. The n-th space-harmonic along the transverse y-axis behaves as $e^{-jk_{yn}|y|}$, where $k_{yn} = \sqrt{k_0^2 - k_{zn}^2}$ is the relevant wavenumber which can have proper or improper spectral determination (negative or positive sign for $\mathfrak{Im}(k_{yn})$, respectively) [22].

III. Tunable periodic GCDR LWAs: TM fields

The modal dispersion behavior of the TM field propagating along the periodic chain of GCDRs is here investigated. The

This article has been accepted for publication in IEEE Antennas and Wireless Propagation Letters. This is the author's version which has not been fully edited and content may change prior to final publication. Citation information: DOI 10.1109/LAWP.2024.3435408

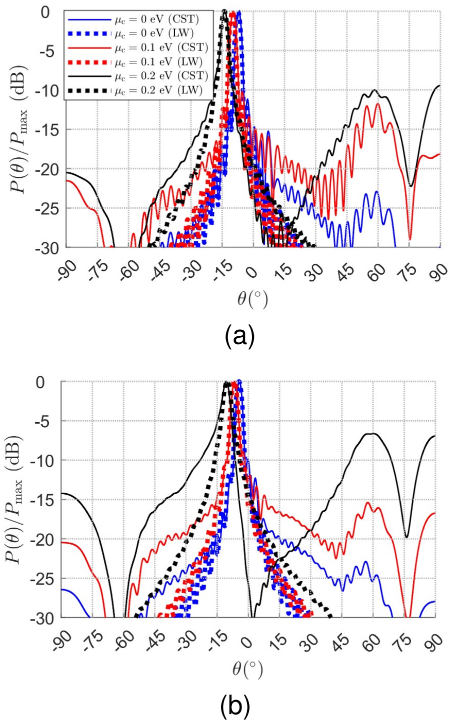

Fig. 3. (a) and (b) TM normalized radiation patterns for periodic GCDR LWAs with parameters as in Fig. 2 at $f = 1.18$ THz and $f = 1.21$ THz for $\tau = 1$ ps and $\tau = 0.5$ ps, respectively.

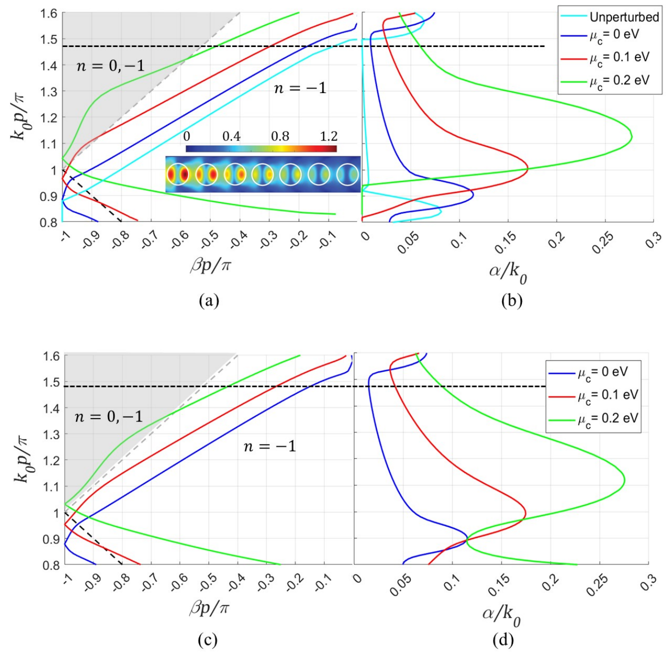

Fig. 4. Same as in Fig. 2 but for the TE modes. In (a) the amplitude of the E_x leaky modal field is reported for $\mu_c = 0.1$ eV at the operating frequency.

dielectric cylinders have a relative permittivity $\epsilon_r = 2.25$ and a radius $r = 0.4167p$. In Figs. 2(a) and 2(b) the Brillouin diagram [26] with the normalized phase constant $\beta p/\pi$ for the $n = -1$ harmonics and the relevant normalized attenuation constant α/k_0 versus the normalized frequency k_0p/π are shown, respectively, for the case $\tau = 1$ ps. Three different values of the chemical potential, namely, $\mu_c = 0, 0.1, 0.2$ eV, are considered to investigate the tunability of the structure. A comparison with the same periodic chain of *bare* (i.e., no graphene) cylindrical dielectric rods (DRs) [22], is also demonstrated. By increasing the frequency above the stopband region $\beta p/\pi \cong -1$, the phase constants of the DRs and GCDRs with $\mu_c = 0, 0.1$ eV lie below the light gray dashed line in the fast-wave region (FWR), representing the scanning behavior of the single beam due to the $n = -1$ space-harmonic in the backward quadrant [26]. The green curve relevant to the case $\mu_c = 0.2$ eV shows a physically different behavior just above the stopband. In fact, the green solid line in Fig. 2(a), within a narrow range right above $k_0p/\pi = 1$, is in the dashed region of the Brillouin diagram where grating lobes occur [26]. Here, both the $n = 0$ improper and $n = -1$ proper harmonics radiate in free space with two distinct beams in the forward and backward quadrants, respectively, which is typically an undesired feature for antenna applications. The normalized attenuation constants in Fig. 2(b) present values that increase considerably with the chemical potential in the frequency region corresponding to the FWR. Hence, in order to avoid the occurrence of the grating lobes and open-stopband effects, maximize the bias-scanning angular range, and obtain sufficiently low values of the leakage constant (i.e., increase peak directivity), a normalized frequency around $k_0p/\pi = 1.51$ is chosen.

In Figs. 2(c) and 2(d) the same results are reported but for $\tau = 0.5$ ps. We observe that the extreme green curve with $\mu_c = 0.2$eV is almost everywhere below the shadowed region in Fig. 2(c), thus making this configuration more robust with respect to grating-lobe occurrence. However, the average values of the attenuation constants are greater than in case of $\tau = 1$ ps and this implies wider beamwidths and lower directivities for the tunable LWA. An operating frequency of $k_0p/\pi = 1.55$ can be here chosen to maximize directivity and beam scanning.

A 3-D tunable LWA is designed on the basis of the present leaky mode analysis. The GCDRs are sandwiched between two plates that behave as perfect magnetic conductors (PMCs) at the chosen operating frequency (see Fig. 1). (Suitable metasurfaces exhibiting a vanishing tangential magnetic field in a narrow band can be properly adopted for this purpose, as shown in, e.g., [27], [28].) The distance between PMC plates is slightly less than the half operating wavelength ($h = 120$ μm) to avoid excitation of higher-order modes neglected by the adopted 2-D approach. Geometrical parameters of the LWA are chosen in order to operate in the low THz range where graphene presents acceptable electromagnetic properties for antenna applications [8]. In particular, a distance between the adjacent rods (i.e., the period) p is fixed to 192 μm and, hence, the radius of the rods is $r = 80$ μm. This leads to an operating frequency $f = 1.18$ THz when $k_0p/\pi = 1.51$ for $\tau = 1$ ps and $f = 1.21$ THz when $k_0p/\pi = 1.55$ for $\tau = 0.5$ ps. In both cases the structure is fed by a parallel plate waveguide with PMC walls supporting the TEM mode with the magnetic field aligned to the cylinder axes (the width of the waveguide and of the PMC plates is $w = 256$ μm). The port is placed in the middle between two adjacent cylinders, where the local maximum for the leaky modal H_x field in Fig. 2(c) is observable. The normalized far-field radiation patterns

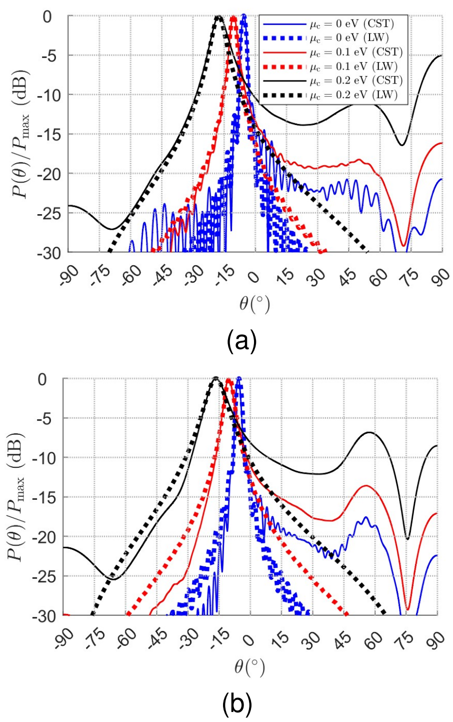

Fig. 5. (a) and (b) TE normalized radiation patterns for periodic GCDR LWAs with parameters as in Fig. 2 at $f = 1.16$ THz for $\tau = 1$ ps and $\tau = 0.5$ ps.

evaluated for three different values of the chemical potential, i.e., $\mu_c = 0, 0.1, 0.2$ eV, are reported in Figs. 3(a) and (b), for $\tau = 1$ ps and $\tau = 0.5$ ps, respectively. The lengths L of the structures have been chosen in order to radiate the 85% and 95% of the injected power for the lowest values of the leakage constant and a length of $25p$ is fixed in both cases. Only angles, measured from the positive y-axis, ranging from $-90°$ to $+90°$, through $0°$, will be shown since the examined structure is symmetric with respect to the $y = 0$ plane. In all cases an excellent agreement for the main beam in the backward quadrant between the radiation patterns of 3-D LWAs simulated with CST [29] and those obtained by using theoretical leaky-wave formulas for truncated structures (adopting a physical-optics approach [19]), is observed. By increasing the chemical potential from 0 eV to 0.2 eV the main beam scans from $-7.1°$ to $-13.8°$, with a directivity that varies from 16 dBi to 13 dBi, and from $-4.3°$ to $-10.5°$, with a directivity from 16 dBi to 10 dBi, for $\tau = 1$ ps and $\tau = 0.5$ ps, respectively. Sidelobe effects due to the occurrence of grating lobes in the forward quadrants are present, which become more evident when the chemical potential increases. Wider beamwidths, as well as a discrepancy between the total CST and the leaky-wave pattern, are observed when $\tau = 0.5$ ps and for higher chemical potentials, as can be predicted by the increasing trend of the leakage constant in Fig. 2 [30].

IV. Tunable periodic GCDR LWAs: TE fields

The dispersion behaviors for modal TE fields are shown in Fig. 4 (for the same geometrical and physical parameters as those for the TM polarization in Sec. III). In the Brillouin diagram in Fig. 4 (a) at $\tau = 1$ ps, we observe that already for moderate high values of the chemical potential, e.g., $\mu_c = 0.2$ eV, the possibility of obtaining a single beam and avoiding grating lobes is limited to the high-frequency region. However, the phase constant dispersion curves are widely spaced for the three different values of μ_c, thus allowing for an increased scanning behavior at fixed frequency with respect to the TM polarization. In addition, also the relevant normalized attenuation constants show moderately higher values in the FWR with respect to those observable in Fig. 2(b). Both these results can be justified by the amplitude of the E_x component of the modal field with maxima placed around the graphene sheet, as shown in Fig. 4(a). This suggests to choose the operating frequency of the tunable LWA close to the minimum preceding the open stopband for the case of $\mu_c = 0$ eV (i.e., at $k_0 p/\pi = 1.48$). By decreasing the relaxation time to 0.5 ps (see Figs. 4(c) and 4(d)), the stopbands around $\beta p/\pi = -1$ become narrower, whereas a moderate increase of the attenuation constant is observable for all the cases studied. The best choice for scanning a beam at fixed frequency by varying μ_c for this leaky-wave structure is again around the minimum of the leakage constant at high frequency for the case of $\mu_c = 0$ eV (i.e., at $k_0 p/\pi = 1.48$).

The 3-D tunable LWA, designed on the basis of the present leaky-mode analysis, is shown in Fig. 1, where the GCDRs are sandwiched between two PEC plates separated by less than the half operating wavelength. The same geometrical and physical parameters as in the TM case, except $h = 125$ μm and $w = 250$ μm, are chosen, thus leading to an operating frequency $f = 1.16$ THz when $k_0 p/\pi = 1.48$ for both $\tau = 1$ ps and $\tau = 0.5$ ps. A rectangular waveguide operating in the TE_{10} mode feeds the LWAs. The normalized far-field radiation patterns evaluated for three different values of the chemical potential, i.e., $\mu_c = 0, 0.1, 0.2$ eV, are reported in Figs. 5(a) and 5(b), for $\tau = 1$ ps and $\tau = 0.5$ ps, respectively. The theoretical leaky-wave radiation efficiency is above 87% and 97% for the two relaxation times. An excellent agreement is shown for the main beam in the backward quadrant between the radiation patterns of the 3-D LWAs simulated with CST and the theoretical leaky-wave patterns. A scanning range of $12.7°$, with pointing angles from $-5.6°$ to $-17.3°$, and directivity from 19 dBi to 11 dBi, is obtained for $\tau = 1$ ps by increasing the chemical potential to 0.2 eV, whereas a beam scanning of $10.8°$, from $-5.8°$ to $-16.6°$, with a directivity ranging from 16.5 dBi to 9.5 dBi, is observed when $\tau = 0.5$ ps. Spurious radiation mainly due to grating lobe effects are visible in the forward quadrant with maximum levels obtained when $\mu_c = 0.2$ eV for $\tau = 1$ ps.

V. Conclusion

Tunable radiation from a periodic chain of graphene-coated dielectric rods is investigated by using a rigorous ad-hoc full-wave modal solver. An accurate modal analysis has been performed for two different values of the relaxation time as the chemical potential varies. Suitable choices of the operating frequencies in the low THz region have been made that maximize the dynamic of the beam scanning by minimizing undesired grating lobe phenomena for both polarizations. Three-dimensional structures simulated with commercial software have shown a very good agreement with the leaky-wave theory giving rise to consistent beam scanning and high directivities.

REFERENCES

[1] M. Esquius-Morote, J. S. Gómez-Díaz, and J. Perruisseau-Carrier, "Sinusoidally modulated graphene leaky-wave antenna for electronic beamscanning at THz," *IEEE Trans. THz Sc. Technol.*, vol. 4, no. 1, pp. 116–122, Jan. 2014.

[2] J. S. Gómez-Díaz, M. Esquius-Morote, and J. Perruisseau-Carrier, "Plane wave excitation-detection of non-resonant plasmons along finite-width graphene strips," *Opt. Express*, vol. 21, no. 21, pp. 24 856–24 872, 2013.

[3] W. Fuscaldo, P. Burghignoli, P. Baccarelli, and A. Galli, "Graphene Fabry-Perot cavity leaky-wave antennas: Plasmonic versus nonplasmonic solutions," *IEEE Trans. Antennas Propag.*, vol. 65, no. 4, pp. 1651–1660, Apr. 2017.

[4] D. Correas-Serrano, J. S. Gómez-Díaz, A. Alù, and A. Á. Melcón, "Electrically and magnetically biased graphene-based cylindrical waveguides: Analysis and applications as reconfigurable antennas," *IEEE Trans. THz Sci. Technol.*, vol. 5, no. 6, pp. 951–960, Jun. 2015.

[5] X.-C. Wang, W.-S. Zhao, J. Hu, and W.-Y. Yin, "Reconfigurable terahertz leaky-wave antenna using graphene-based high-impedance surface," *IEEE Trans. Nanotechnol.*, vol. 14, no. 1, pp. 62–69, Jan. 2015.

[6] M. Gao, K. Li, F. Kong, G. Zhu, and H. Zhuang, "Graphene-based terahertz closed-stopband tunable composite right/left-handed leaky-wave antennas," *Optical and Quantum Electronics*, vol. 53, no. 470, 2021.

[7] W. Fuscaldo, P. Burghignoli, P. Baccarelli, and A. Galli, "A reconfigurable substrate-superstrate graphene-based leaky-wave THz antenna," *IEEE Antennas Wireless Propag. Lett.*, vol. 15, pp. 1545–1548, 2016.

[8] ——, "Graphene terahertz leaky-wave antennas," in *Handbook of Graphene, Volume 8: Graphene Technology and Innovation*, S. Arun, Ed. Hoboken, NJ: John Wiley & Sons, 2019, ch. 10, pp. 309–340.

[9] M. Saeed, A. Ghaffar, S. U. Rehman, M. Y. Naz, S. Shukrullah, and Q. A. Naqvi, "Graphene-based plasmonic waveguides: A mini review," *Plasmonics*, vol. 17, no. 3, pp. 901–911, 2022.

[10] D. Teng, K. Wang, and Z. Li, "Graphene-coated nanowire waveguides and their applications," *Nanomaterials*, vol. 10, no. 2, p. 229, 2020.

[11] Y. Kou and J. Förstner, "Discrete plasmonic solitons in graphene-coated nanowire arrays," *Optics Express*, vol. 24, no. 5, pp. 4714–4721, 2016.

[12] P. Meng, D. Zhao, D. Zhong, and W. Liu, "Topological plasmonic modes in graphene-coated nanowire arrays," *Optical and Quantum Electronics*, vol. 51, pp. 1–10, 2019.

[13] S. V. Dukhopelnykov, M. Lucido, R. Sauleau, and A. I. Nosich, "Circular dielectric rod with conformal strip of graphene as tunable terahertz antenna: interplay of inverse electromagnetic jet, whispering gallery and plasmon effects," *IEEE Journal of Selected Topics in Quantum Electronics*, vol. 27, no. 1, pp. 1–8, Jan. 2020.

[14] A. Y. Svezhentsev, A. I. Nosich, V. Volski, and G. A. Vandenbosch, "THz range natural modes and scattering resonances of circular dielectric micro-cylinder covered with graphene: The H-polarization case," *Opt. Quantum Electron.*, vol. 55, no. 3, p. 253, 2023.

[15] P. Yu, V. I. Fesenko, and V. R. Tuz, "Dispersion features of complex waves in a graphene-coated semiconductor nanowire," *Nanophotonics*, vol. 7, no. 5, pp. 925–934, 2018.

[16] H. Soleimani and H. Oraizi, "Sinusoidally modulated leaky wave antenna based on cylindrical graphene waveguide," *JOSA B*, vol. 36, no. 11, pp. 3189–3195, 2019.

[17] ——, "Plasmonic leaky wave antenna based on modulated radius of cylindrical graphene waveguide," *AIP Advances*, vol. 11, no. 9, 2021.

[18] W. Fuscaldo, P. Burghignoli, P. Baccarelli, and A. Galli, "Efficient 2-D leaky-wave antenna configurations based on graphene metasurfaces," *Int. J. Microwave Wireless Techn.*, vol. 9, no. 6, pp. 1293–1303, 2017.

[19] D. R. Jackson and A. A. Oliner, "Leaky-wave antennas," in *Modern Antenna Handbook*, C. A. Balanis, Ed. Hoboken, NJ: John Wiley & Sons, 2008, ch. 7, pp. 325–367.

[20] A. A. Oliner and D. R. Jackson, "Leaky-wave antennas," in *Antenna Engineering Handbook*, J. L. Volakis, Ed. New York, NY: McGraw-Hill, 2007, ch. 11.

[21] V. Jandieri, P. Baccarelli, G. Valerio, and G. Schettini, "1-D periodic lattice sums for complex and leaky waves in 2-D structures using higher order Ewald formulation," *IEEE Trans. Antennas Propag.*, vol. 67, no. 4, pp. 2364–2378, Apr. 2019.

[22] V. Jandieri, P. Baccarelli, G. Valerio, K. Yasumoto, and G. Schettini, "Modal propagation in periodic chains of circular rods: Real and complex solutions," *IEEE Photon. Techn. Lett.*, vol. 32, no. 17, pp. 1053–1056, Sep. 2020.

[23] K. Yasumoto, *Electromagnetic theory and applications for photonic crystals*. Boca Raton, FL: CRC Press, 2018.

[24] V. P. Gusynin, S. G. Sharapov, and J. P. Carbotte, "On the universal AC optical background in graphene," *New J. Phys.*, vol. 11, no. 9, p. 095013, 2009.

[25] W. Zouaghi, D. Voß, M. Gorath, N. Nicoloso, and H. G. Roskos, "How good would the conductivity of graphene have to be to make single-layer-graphene metamaterials for terahertz frequencies feasible?" *Carbon*, vol. 94, pp. 301–308, 2015.

[26] P. Baccarelli, S. Paulotto, D. R. Jackson, and A. A. Oliner, "A new Brillouin dispersion diagram for 1-D periodic printed structures," *IEEE transactions on Microwave Theory and Techniques*, vol. 55, no. 7, pp. 1484–1495, 2007.

[27] O. Luukkonen, C. Simovski, G. Granet, G. Goussetis, D. Lioubtchenko, A. V. Raisanen, and S. A. Tretyakov, "Simple and accurate analytical model of planar grids and high-impedance surfaces comprising metal strips or patches," *IEEE Trans. Antennas Propag.*, vol. 56, no. 6, pp. 1624–1632, Jun. 2008.

[28] W. Fuscaldo, D. C. Zografopoulos, F. Imperato, P. Burghignoli, R. Beccherelli, and A. Galli, "Analysis and design of tunable THz 1-D leaky-wave antennas based on nematic liquid crystals," *Appl. Sci.*, vol. 12, no. 22, p. 11770, 2022.

[29] "SIMULIA CST Studio Suite, Dassault Systemes. (2023)." [Online]. Available: https://www.3ds.com/products-services/simulia/products/cst-studio-suite/

[30] T. Tamir and A. Oliner, "Guided complex waves. part 2: Relation to radiation patterns," in *Proceedings of the Institution of Electrical Engineers*, vol. 110, no. 2. IET, 1963, pp. 325–334.